RESEARCH ARTICLE

Preparation of Calcium Phosphate Nanoparticles: Study their Characterization and Antibacterial Activity

Zainab A. Fadhil Al-Mimar[1*], Hussain S. Hasan[1], Ghassaq Tariq Al-Ubaidi[2]

[1]*Department of Physiology and Medical Physics, College of Medicine, Al-Nahrain University, Kadhimiya, Baghdad, Iraq*
[2]*Medical Research Unit, College of Medicine, Al-Nahrain University, Kadhimiya, Baghdad, Iraq*

Received: 26th June, 2020; Revised: 25th July, 2020; Accepted: 19th August, 2020; Available Online: 25th September, 2020

ABSTRACT

Calcium phosphate nanoparticles (CPNPs) have been synthesized by chemical precipitation method and were characterized by UV-visible spectroscopy (UV-vis), Fourier transform infrared spectroscopy (FTIR), and scanning electron microscopy (SEM). The antibacterial activity against multi-drug resistant (MDR) gram-negative bacteria *Pseudomonas aeruginosa (P. aeruginosa)* and *Klebsiella pneumonia (K. pneumonia)* was performed by well diffusion method, using different concentrations of CPNPs and different combinations of CPNPs with ciprofloxacin (CIP) (CIP-CPNP100, CIP-CPNP50, and CIP-CPNP25). The minimum inhibitory concentration (MIC) and minimum bacterial concentration (MBC) were evaluated by the broth dilution method and optical density. Cytotoxicity of nanoparticles was evaluated by 3-(4,5-dimethylthiazol-2-yl)-2,5-diphenyltetrazolium bromide (MTT) assay on polymorphonuclear cells. Results indicated that synthesized CPNPs sized 28.02 ± 3.2 nm in diameter as average, with distorted spherical shape appears as agglomerates. CPNPs showed no antibacterial activity against MDR bacteria, but combining them with CIP recorded antibacterial activity represented by inhibition zone against MDR bacteria. It was found that the inhibition zone increases when the concentration of CIP and particle size decreases. The MTT assay reveals the acceptable toxicity of the synthesized nanoparticles. The present study can be helpful to formulate nano-drug conjugates as antimicrobial agents in various fields of medical research.

Keywords: Antibacterial, Calcium phosphate, Hydroxiaptite, Multi drug resistant, Nanoparticles.

International Journal of Drug Delivery Technology (2020); DOI: 10.25258/ijddt.10.3.24

How to cite this article: Al-Mimar ZAF, Hasan HS, Al-Ubaidi GT. Preparation of calcium phosphate nanoparticles: study their characterization and antibacterial activity. International Journal of Drug Delivery Technology. 2020;10(3):440-447.

Source of support: Nil.

Conflict of interest: None

INTRODUCTION

The new field of nanotechnology, *viz*., nanomedicine, introduces a rapid change in the medical field by opening a new version that improves human health. Nowadays, nanotechnology is a promising area for solving various problems in health care and medicine. It is still evolving as a new field of medicine that uses nanoparticles in diagnostics, imaging, genes, and drug delivery.[1] Increasing antibiotic resistance in bacterial strains is a serious and growing threat to human health as MDR bacteria cause millions of infections each year. The antibiotic resistance of bacteria is a global health problem that is continually expanding and is recognized as a medical problem that increases morbidity and mortality rates, which implies the length of hospital stays, as well as, cost and bad prognosis.[2] In fact, the speed at which bacteria are establishing resistance to current antibiotics is faster than the development of new molecules with antimicrobial features. Unfortunately, it is very difficult to identify new bacterial targets that can be used to develop new classes of antimicrobial agents that are safe and effective.[3] Nanotechnology opens new possibilities, allowing new solutions with old resources. Nanoparticles have emerged as novel antimicrobial agents owing to their effectiveness in small doses large surface area to volume ratio, minimal toxicity, and lack of side effects.[4] Numerous studies have applied the nanoparticles (NPs) as the drug carriers, some features that nanocarriers can incorporate in drug delivery systems promoted dissolution of drugs, improved solubility and stability, enhanced absorption of drugs, increased drug targeted performance, controlled release capability of drugs, and reduced side effects.[5] As an important inorganic mineral, calcium phosphate (CP) is a natural biomineral, and therefore, possesses excellent biocompatibility due to its chemical similarity to human hard tissue (bone and teeth). Calcium phosphate has been extensively studied throughout the last few decades for their role in bone and teeth mineralization, as well as, in pathological calcifications.[6] Recently, CPNPs have been widely used in biomedical applications due to their good biocompatibility and bioactivity, such as, non-viral gene, drug delivery vectors, and a carrier in biological systems.[7]

**Author for Correspondence: zynb0102@gmail.com*

MATERIAL AND METHODS

Preparation of CPNPs using Chemical Precipitation

CPNPs were synthesized using a chemical precipitation method.[8] A 100 mL of 0.6 M $Ca(NO_3)_2 \cdot 4H_2O$ (Thomas Baker) was vigorously stirred at room temperature, then 100 mL of 0.4 M of $(NH_4)_2HPO_4$ (Thomas Baker) was added dropwise as a reducing agent to $Ca(NO_3)_2 \cdot 4H_2O$ solution for 40 minutes (2.5 mL/min). The pH of the final mixture reaction was adjusted to 10 by adding 200 mL of 0.1 M of sodium hydroxide (Thomas Baker), which acts as a precipitating agent through the stirring process. The mixture was left under a magnetic stirrer overnight. A white precipitate appeared in the beaker. The precipitate was vacuum dried and washed by distilled water five times, then it was further dried in an electric oven at a temperature of 40ºC for 5 hours.

Characterization of CPNPs

By UV-Vis Spectrophotometer Spectroscopy

The preliminary detection of the formation of CPNPs was done in UV-visible spectrophotometer (Shimadzu UV-1800, Japan), by scanning the absorbance spectra of the solution in the range 285 to 600 nm.[6]

By Fourier Transform Infrared Spectroscopy (FTIR)

The FTIR spectroscopy (Alpha Platinum-ATR) is a widely used approach that identifies functional groups of the NPs with the use of infrared radiation beams. An infrared spectroscopy measures infrared radiation absorption, which is made with every one of the bands in the molecule, thus, provides a spectrum that is applied as percent transmittance (%) *vs.* wavenumber (cm^{-1}); infrared spectra used in the wave range of 400–4,000 cm^{-1}.[9]

By SEM

The SEM (LEO 982 SEM) is utilized to determine the size, shape, and morphology of the produced nanoparticles through the magnification power of 200.kx.[10]

Preparation of NPs-Antibiotic Combinations

The CIP solution prepared as 25 mg/mL with distilled water, CIP-CPNPs combinations were prepared in different weight ratios (WR) of 1:4, 1:2, and 1:1, for CIP-CPNP100, CIP-CPNP50, and CIP-CPNP25, respectively. The reaction was conducted under continuous magnetic stirred for 3 hours at room temperature, then the solutions left undisturbed overnight. Those samples were subjected to characterization by SEM and FTIR by adding a few drops of these solutions on the slide and left to dry at room temperature.

Antibacterial Assay

The bacterial isolates were collected from Al-Imamain Alkadhimain Medical City, Baghdad, Iraq. The two bacterial species were identified as MDR, depending on antibiotic susceptibility testing, using the disk diffusion method. The antibacterial activity of bare CPNPs and CIP-CPNP (100, 50, and 25) were tested against gram-negative bacteria *P. areuginosa and K. pneumoniae* by well diffusion method. The inoculum density was adjusted according to 0.5 McFarland standard, then placed on mueller hinton agar (MHA) plates in a heavy streaking pattern by sterilized loops and left for 2 to 3 minutes to dry. Wells (8 mm) were punched in the plates using a sterile steel cork borer. 100 µL from each concentration CPNPs (25, 15, 10, and 5 mg/mL) and CIP-CPNP (100, 50, and 25) poured in wells and incubated at 37ºC/24 hours. The diameter of the inhibition zone was measured and expressed in mm, and the experiment was conducted in triplicate.

Minimum Inhibitory Concentration (MIC)

The MIC is defined as the minimum concentration of the tested material that inhibits bacterial growth. This can be achieved via the double broth dilution method and optical density. 2 mL of CIPNP100 was diluted as two-fold dilutions (1/2, 1/4, 1/8, 1/16, and 1/32) in the autoclave-sterilized Muller Hinton broth. Seven sterile tubes were placed in a rack and labeled (1, 2, 3, 4, 5, 6, and 7). 1-mL of Muller Hinton broth was added to the tubes 1 to 7. With sterile tips, 1-mL of CIP-CPNP100 was added to the second test tube and mixed well by pipetting. 1-mL was transferred from tube number 2 to tube number 3, mixed well to get dilution 1/4; this step is repeated until reach in 1/32 dilution tube number 6. 100 µL of bacterial suspension was inoculated in tubes 1 to 6. Tube number 1 considered as the positive control tube, containing only 1-mL of MHB and bacterial suspension without CIP-CPNP100. Tube number 7 is the negative control tube, containing 1-mL of mueller hinton broth (MHB) and 1-mL of CIP-CPNP100. All 7 tubes were incubated at 37ºC/24 hours. To examine bacterial growth, the optical density (OD) of each tube was measured on wavelength 600 nm.

Minimum Bactericidal Concentration (MBC)

This test is complementary to the MIC. MBC is defined as the lowest concentration that is required to completely prevent bacterial growth on a solid medium. This test is conducted through a full loop of each tube of MIC that was subcultured on MHA plates. Plates were incubated at 37ºC/24 hours.

Detection of CPNPs Cytotoxicity to Human Primary Cells

The viability of cells treated with CPNPs and CIP-CPNP was determined by MTT assay.[11] Medium of RPMI-1640 was prepared according to manufactured, supplemented with L-glutamine, 25mM, (4-(2-hydroxyethyl)-1-piperazineethane sulfonic acid) 1% penicillin-streptomycin, and 10% of fetal calf serum (FCS) was preheated at 56ºC/30 minutes for inactivation. The polymorphonuclear cells were isolated from a volunteer blood sample, was collected in a heparinized tube, and cells were isolated using Ficoll-Paque. The layers of polymorphonuclear cells were aspirated by a sterilized tip. The primary cells (polymorphonuclear cells) were cultured in the RPMI medium, incubated at 37ºC in 5% CO_2. After 48 hours of incubation, cell growth was examined to get a confluent monolayer. The MTT stain as 4 mg/10 mL was prepared in phosphate buffer saline (PBS); the solution was filtered by a 0.22 µM filter unit. In a sterilized 96-well plate, 100 µL of polymorphonuclear cells were cultured and

incubated overnight at 37ºC. 100 µL of CPNPs (25, 15, 10, and 5 mg/mL), and CIP (CIP-CPNP100, CIP-CPNP50, and CIP-CPNP25) were added to the first well of each row and incubated at 37ºC/48 hours. To each well, 28 µL of 2 mg/mL of MTT solution was added, cells were incubated at 37ºC for 1.5 hours. The MTT solution was aspirated, crystals remain in wells were solubilized by adding 130 µL of dimethyl sulphoxide (DMSO), followed by incubation at 37ºC/15 minutes, with shaking. The cell viability was detected by measuring OD at 492 nm using a spectrophotometer. The cell viability was calculated by using the following equation:

$$\text{Cell viability (\%)} = (\text{OD sample/OD control}) \times 100 \quad (1)$$

Statistical Analyses

Statistical analyses were performed using SPSS software version 16.0 (SPSS, Chicago, IL, USA). Analysis of variance (ANOVA) test was used to compare means between different groups. A p-value of 0.05 or less was considered statistically significant.

RESULTS

CPNPs Characterizations

UV-Vis Spectrophotometer Spectroscopy Results

The prepared solution of CPNPs was analyzed using scanning UV-vis spectroscopy, with wavelength values ranging from 285 to 600 nm. Results showed that the maximum absorbance of synthesized CPNPs was 0.916 at wavelength 296 nm, indicating that maximum λ is observed within the UV-vis region (Figure 1).

FTIR Data Analysis

The chemically synthesized CPNPs were analyzed by Alpha Platinum-ATR FTIR, UK. The FTIR spectra showed the characteristic absorption peaks of CPNPs (Figure 2). The sample spectra showed the characteristic bands; the band was observed at 3,499.21 cm^{-1} to the stretching mode vibration of the hydroxyl group (OH^-), respectively, bands at 1,020.98, 599.23, and 560.44 cm^{-1}, are attributed to the phosphate group (PO_4^{3-}). Three bands at 3,383.75, 1725.22, and 1645.49 cm^{-1} are attributed to water molecules. In addition, carbonate content was seen, CO_3^{2-} peaks were detected at 1,521.83 cm^{-1}, indicating the presence of carbonate apatite. According to this spectra, it is clear that the chemically synthesized powder is certainly nano-hydroxyapatite (n-HAP).

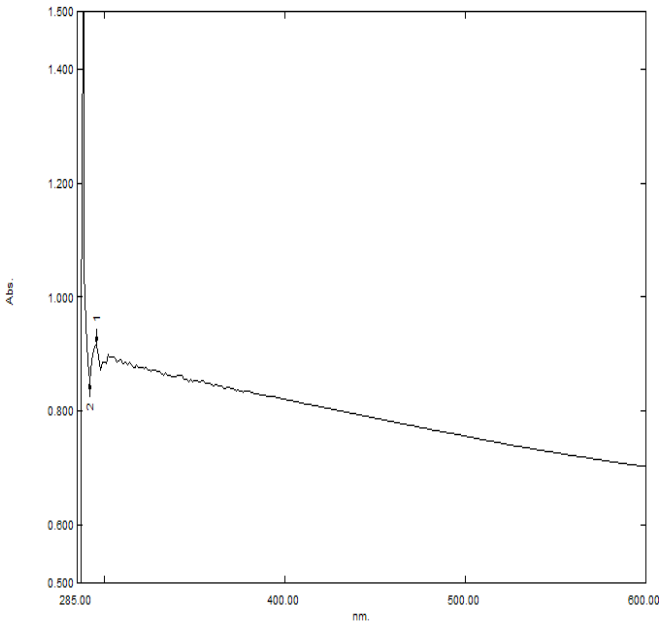

Figure 1: UV-vis spectrum for CPNPs

Scanning Electron Microscopy

The synthesized CPNPs were analyzed by LEO 982 SEM to determine size, shape, and morphology. Observations on magnification power 200 kx and 1.04 µm view field showed the presence of distorted spherical NPs ranging in size 23.81 to 32.74 nm in diameter, with a mean size of 28.02 ± 3.2 nm. Agglomerates consisting of several NPs were observed; it is obvious that CPNPs are coarse and exhibited protuberances on their surfaces (Figure 3).

CIP-CPNPs Combinations Characterizations

Combinations of CIP and CPNPs were prepared in three different WR, i.e., 1:1, 1:2, and 1:4, *viz.*, CIP-CPNP25, CIP-CPNP50, and CIP-CPNP100, respectively, and were

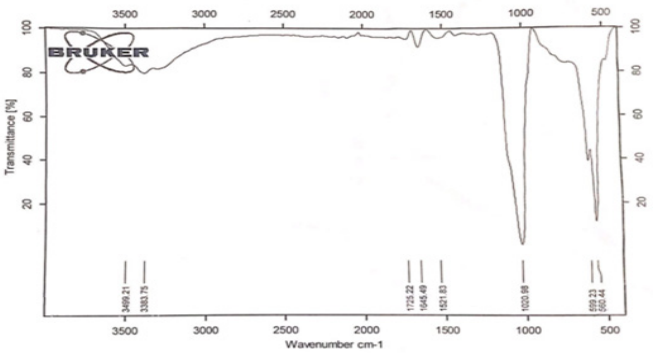

Figure 2: FTIR spectrum of synthesized CPNPs

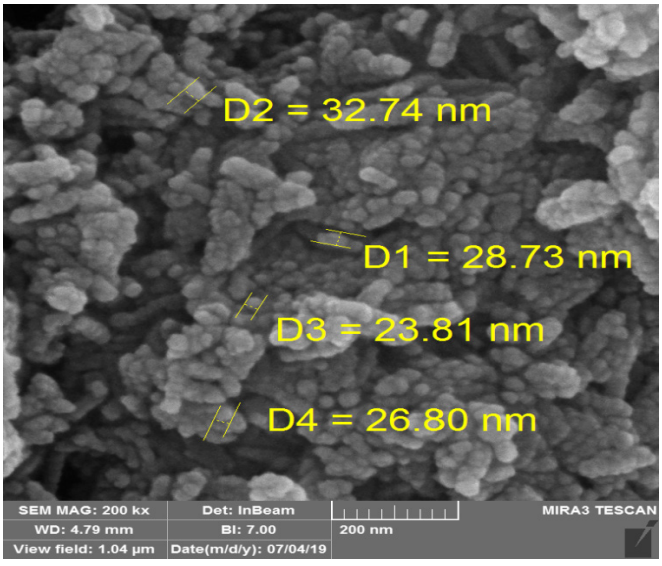

Figure 3: SEM images of bare CPNPs with magnification power 200 kx

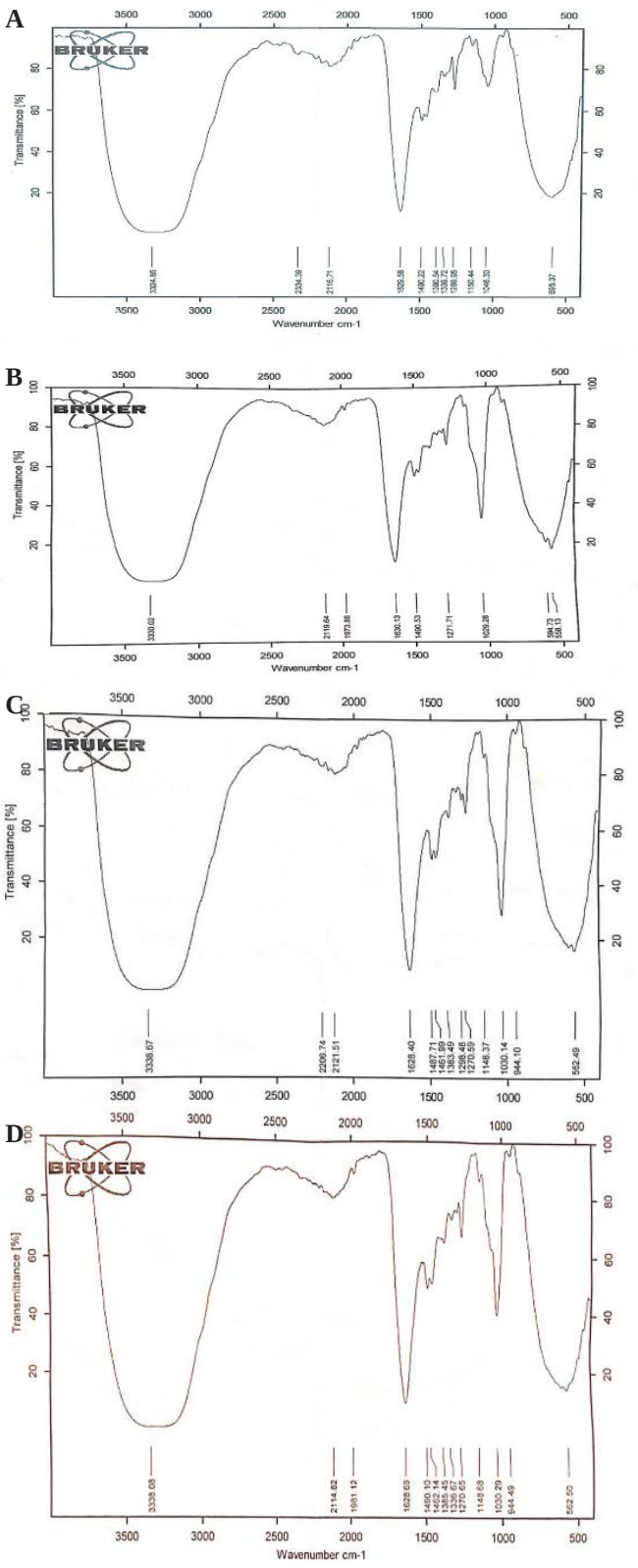

Figure 4: FTIR of **A:** CIP; **B:** CIP-CPNP100; **C:** CIP-CPNP50; **D:** CIP-CPNP25

characterized by FTIR and SEM to verify the conjunction success.

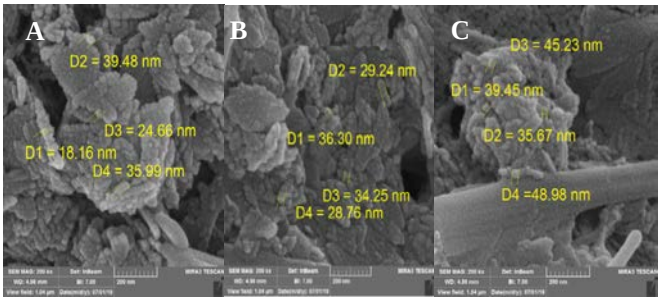

Figure 5: SEM image with magnification power 200 kx of **A:** CIP-CPNP100 (1:4 WR); **B:** CIP-CPNP50 (1:2 WR); **C:** CIP-CPNP25 (1:1 WR)

FTIR Spectroscopy of CIP-CPNP

The interaction of CIP with CPNPs was studied by FTIR analysis. The typical FTIR of CIP, CIP-CIPNP100, CIP-CIPNP50, and CIP-CIPNP25 are presented in Figure 4. Regarding the FTIR spectra of CIP, visible peaks appear at a frequency of 3,330.02 cm^{-1}, ascribed to hydroxyl group stretching mode vibration, and 1,271.71 cm^{-1} assigned to bending vibration of the hydroxyl group. The characteristics peaks at 1,630.13 and 1,029.28 cm^{-1}, ascribed to the stretching vibration of the quinoline group and stretching vibration of the fluorine group, respectively. While, the chrematistics peak at 1,490.53 cm^{-1} was assigned to stretching vibration of the carbonyl group. Regarding the FTIR spectra of CIP-CPNP100, CIP-CPNP50, and CIP-CPNP25, the characteristic peaks are almost the same as that of CIP.

SEM of CIP-CPNP

Qualitative analysis of NPs behavior and morphology was studied by SEM. Results reveal that CIP-CPNP100 in 1:4 WR gave the smallest size, mean size 29.98 ± 9.8 nm, followed by CIP-CPNP50 in 1:2 WR and CIP-CPNP25 in 1:1 WR, 32.69 ± 6.1 and 42.3 ± 5.9 nm, respectively. That means increment in CIP concentration will increase the size of the nanoparticles. A significant difference was detected in NPs' size between CIP-CPNP100 and CIP-CPNP25 p value < 0.05. Also, there is a significant difference between bare CPNP and bare CIP-CPNP25, p-value < 0.05, while, no significant differences were detected among other studied groups, p-value < 0.05. Regarding the morphology of CPNPs conjugated to CIP, it is obvious that those conjugated with CIP (100, 50, and 25) showed to appear in bigger agglomerates, and particle shape looks less distorted as compared to bare CPNPs (Figure 5).

Antibacterial Activity

Antibacterial Activity of different Concentrations of Bare CPNPs

The two isolates of bacteria were identified as resistant to CIP, depending on antibiotics susceptibility testing, using the disk diffusion method. The antibacterial activity of different concentrations of bare CPNPs (25, 15, 10, and 5 mg/mL) was evaluated against the two MDR isolates, *P. areuginosa*, and *K. pneumoniae*, using the well diffusion method. Results revealed the absence of antibacterial activity

Table 1: Inhibition zone for CIP-CPNP100, CIP-CPNP50, and CIP-CPNP25 against two bacteria studied

Bacteria	*CIP-CPNP100*	*CIP-CPNP50*	*CIP-CPNP25*	*p value*
P. areuginosa	22.33 ± 0.58[a]	21.67 ± 0.58[a]	15.67 ± 0.58[b]	< 0.001
K. pneumoniae	25.56 ± 0.58[a]	25.33 ± 0.58[a]	16.67 ± 0.58[b]	< 0.001

Note: Different small letters ([a] and [b]) noticed in Table 1, indicate exiting significant differences between the above three groups

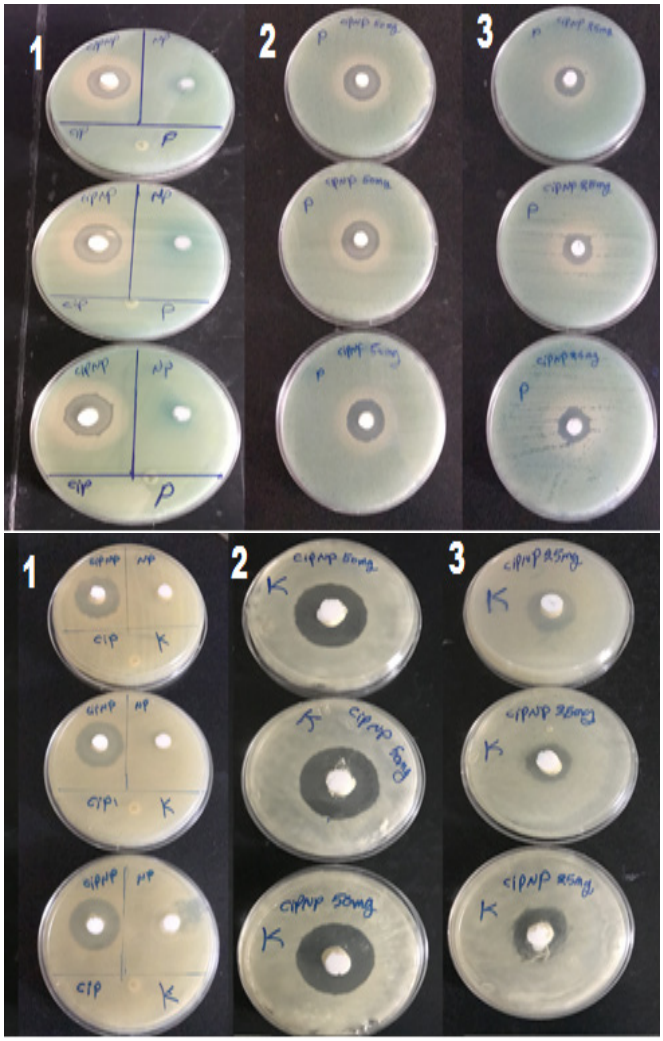

Figure 6: Antibacterial activity against **A:** *P. areuginosa*; **B:** *K. pneumoniae*; for 1: CIP-CPNP100, 2: CIP-CPNP50, and 3: CIP-CPNP25

for CPNPs against the two isolates studied even at the highest concentration.

Antibacterial Activity of different Concentrations of CIP-CPNP Combinations

The three CIP-CPNPs combinations 1:1, 1:2, and 1:4 (i.e., CIP-CPNP25, CIP-CPNP50, and CIP-CPNP100), respectively, were verified for their antibacterial activity against gram-negative bacteria *P. areuginosa* and *K. pneumoniae*, using the well diffusion method. Regarding gram-negative bacteria, *P. aeruginosa* showed 22.33 ± 0.58, 21.67 ± 0.58, and 15.67 ± 0.58 mm inhibition zone for CIP-CPNP100, CIP-CPNP50, and CIP-CPNP25, respectively (Figure 6A). While, *K. pneumoniae* showed 25.56 ± 0.58, 25.33 ± 0.58, and 16.67 ± 0.58 mm inhibition zone for CIP-CPNP100,

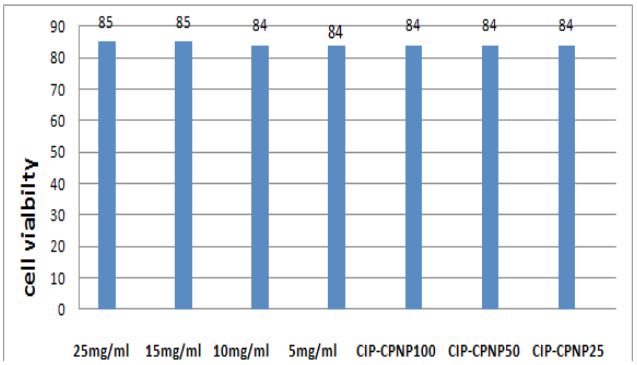

Figure 7: MTT assay shows primary cells viability after challenging with CPNPs and different combinations of CIP

CIP-CPNP50, and CIP-CPNP25, respectively (Figure 6B). Moreover, CIP and CPNPs don't have antibacterial activity, only when they delivered together. From the results mentioned above, a highly significant difference in antibacterial activity was detected in CIP-CPNP25 comparing to treated CIP-CPNP100, and CIP-CPNP50, $p < 0.001$, for the two studied isolates. While, no significant difference in antibacterial activity was detected between CIP-CPNP100 and CIP-CPNP50 for the two studied isolates, $p > 0.05$ (Table 1).

Minimum Inhibitory Concentration (MIC) and Minimum Bacterial Concentration (MBC)

The CIP-CPNP100 was diluted by the double dilution method in five dilutions (1/2, 1/4, 1/8, 1/16, and 1/32), final CIP-CPNP100 concentration in each dilution was 12.5-50, 6.25-25, 3.12-12.5, 1.56-6.25, and 0.78-3.12 mg/mL, respectively. After 24 hours of incubation at 37ºC, results revealed that 1.56-6.25 mg/mL of CIP-CPNP100 is the MIC for *P. areuginosa* and *K. pneumoniae*. The MBC was determined to be 3.12-12.5 mg/mL for *P. areuginosa* and *K. pneumoniae.*

Cytotoxicity of CPNPs to Polymorphonuclear Cells

It was attempted to determine the CPNPs' cytotoxic effect on human polymorphonuclear cells. The MTT assay was applied to detect cell viability by measuring the absorbency on a microtiter plate reader at 492 nm wavelength.

The non-treated polymorphonuclear cells represented the control sample. While, other samples are represented by cells treated with four different concentrations of bare CPNPs (25, 15, 10, and 5 mg/mL), and other cells treated with CIP-CPNP100, CIP-CPNP50, and CIP-CPNP25. It was found that cells viability for non-treated cells was 100% , cell viability percentage were found of other samples as 85, 85, 84, and 84% for polymorphonuclear cells treated with CPNPs (25, 15, 10, and 5 mg/mL), respectively. Also, cell viability was 84% for polymorphonuclear cells treated with different combinations of CIP-CPNP (CIP-CPNP100, CIP-CPNP50,

and CIP-CPNP25). Those results indicate that CPNPs are biocompatible material and posses no cytotoxic effect. Also, the addition of ciprofloxacin did not increase or decrease its cytotoxic effect (Figure 7).

DISCUSSION

CPNPs are good candidates for drug delivery since they are easy to synthesize and inexpensive. They are also recognized by good biocompatibility and biodegradability.[12] In the present work, CPNPs are prepared in a chemical precipitation method. This method is very simple, produces nanoparticles in large quantities, and with high reproducibility. For the characterization of the prepared CPNPs, the following techniques were used, *viz*., UV-vis, FTIR, and SEM. The maximum absorbance of prepared CPNPs in the present work was recorded at wavelength 296 nm that is compatible with 295 nm that was recorded by Al-Ubaidi in 2018, who prepared colloidal CPNPs using chemical methods also.[13]

The size of the synthesized CPNPs was performed using SEM. The SEM analysis revealed that the prepared CPNPs lie in the nanoscale level with an average particle size of 28.08 ± 3.2 nm. This size is comparable to that produced by Mndal and her coworkers, 23.15 ± 2.56 nm in diameter, using the same preparation method.[11] Another study conducted by Chandrasekar and his colleagues in 2013 prepared CPNPs with size 50 nm, using the same preparation method.[14]

The functional group of CPNPs, observed by FTIR spectra, generated one characteristic peak of stretching mode of the hydroxyl group at 3,499.22 cm^{-1}. The stretching mode peak is similar to stretching mode 3,497 cm^{-1} of the hydroxyl group of HAP NPs, which were prepared by Nithya and Sundaram in 2015, using the precipitation chemical method.[15] The band presented at 1,020.98 cm^{-1} in FTIR spectra are corresponding to the stretching mode of the phosphate group, while bands at 599.23 and 560.44 cm^{-1} are found due to the bending mode of the phosphate group. Peaks of the phosphate group were comparable with peaks at 1,020, 600, and 560 cm^{-1}, introduced by Kojima and his group in 2018.[16] The presence of the above functional group, hydroxyl group, and phosphate group, show the formation of CPNPs in the HAP phase according to Kojima S.[17] The observed peak at 1,521.83 cm^{-1} corresponding to the carbonate group is due to the absorption of CO_2 from the atmosphere.[18] On the contrary, the peaks at 1,645.49, 1,725.22, and 3,383.75 cm^{-1} are attributed to water molecules due to the water adsorption during the synthesis process.[17-19] Regarding the FTIR spectra of CIP, the characteristics peaks at 3,330.02 and 1,271.71 cm^{-1} ascribed to stretching mode vibration and bending mode vibration of the hydroxyl group, respectively. The characteristics peaks at 1,630.13 and 1,029.28 cm^{-1} ascribed to the stretching vibration of the quinoline group and stretching vibration of the fluorine group, respectively. While, the chrematistics peak at 1,490.53 cm^{-1} was assigned to the stretching vibration of the carbonyl group. The presence of the above functional group of CIP is comparable with the functional group of CIP, reported by Sahoo and his team group in 2011 (Sahoo *et al*., 2011). In the FTIR spectra of CIP-CPNP combinations, the characteristic peaks were almost similar to that of CIP, or very slight shifting of these peaks occurred. This confirms the presence of CIP in the CPNPs system with no major peak shifts in the fingerprint region of the CIP FTIR spectra; this is thought to be due to the adsorption of CIP on the surface of CPNPs, which further strengthens the claim that the antibiotics are mostly physisorbed on the NPs' surface.[20-22] Regarding CIP-CPNP combinations (CIP-CPNP100, CIP-CPNP50, and CIP-CPNP25), it was found that the particle sizes are 29.98 ± 9.8, 32.69 ± 6.1, and 42.3 ± 5.9 nm in diameter, respectively, indicating that increment in CIP concentration results in increment in CPNPs' size. This finding is in accordance with other researches. For instance, silver nanoparticles, 51 nm in diameter, were increased in size 61 and 62 nm, when combined with amikacin and vancomycin, respectively.[23] Maleki Dizaj and his group in 2017, reported an increment in the size of calcium carbonate NPs from 89.64 to 116.09 nm, when CIP was added.[24]

Regarding resistance of bacteria to CIP, it may arise as a result of alterations in the target enzymes (DNA gyrase and topoisomerase IV), and/or changes in the efflux system.[25] In the present study, results showed no inhibition zone for all concentrations of CPNPs. This indicates the absence of antibacterial activity of CPNPs. Most researchers verified the absence of such activity for both gram-negative and gram-positive bacteria.[26-28] However, Addition CIP to the CPNPs resulted in both bacterial growth inhibition and bactericidal effect, against both gram-negative and gram-positive bacteria. It seems that CPNPs enhance the CIP entrance to the bacterial cell. This is due to the fact that binding sites of CPNPs are substantially found in the calcium ions (Ca^{2+}), and because the bacterial cell surfaces are negatively charged due to the phosphoryl and carboxylate groups located on the macromolecules of the outer cell envelope. This difference in charge will lead to electrostatic interaction between the CIP-CPNP and the bacterial surface.[29,30] Thus, the CPNPs will enhance the CIP entrance into the bacteria cell, that CIP will act on the target enzymes (DNA gyrase and topoisomerase IV). The antibacterial activity result is comparable with the antibacterial activity result introduced by Pan and his teamwork in 2018, who was able to enhance the antibacterial activity of gentamicin against MDR bacteria, by using calcium carbonate NPs.[31]

In more detail, it is found that low CIP:CPNPs ratios, i.e., 1:4 (CIP:CPNP100) and 1:2 (CIP:CPNP50), gave higher antibacterial activity, comparing to the third combination that encompasses higher concentration of CIP 1:1 (CIP:CPNP25). This is thought to be due to the fact that the first and second combinations, i.e., 1:4 and 1:2, posses significantly smaller size of CPNPs, 29.98 ± 9.8, and 32.69 ± 6.1 nm, respectively, comparing to the third combination, 1:1, 42.3 ± 5.9 nm. It is speculated that this size smallness will result in an increment in surface/volume ratio, which is one of the most important advantages of NPs that will eventually lead to enhancing the adsorption capacity,[32] and thus, will facilitate CIP entrance

into the bacteria cell. Our results may lead to speculation that antibiotic resistance of the three studied bacteria is mostly due to the alteration in the efflux transporters not in the CIP target enzyme, especially, that the recoded resistance is for multiple antibiotics, each one posses different target. By using MTT assays to detect CPNPs cytotoxicity, polymorphonuclear cells treated with CPNPs showed 85 and 84% cell viability even when treated with CPNPs of 25 mg/mL concentrate. Also, it is found that the addition of CIP to CPNPs does not affect the cell viability even at the height:weight ratio 1:4. Results revealed the cell viability of 84% of the cell treated with CIP-CPNP (100, 50, and 25). The results of the cell viability of CPNPs and CIP-CPNP (100, 50, and 25) are in good agreement with the result reported by Zhang and his group in 2012, who found the cell viability of the treated cell with vancomycin-HAP NPs is more than 80% even at the material concentration up to 100 mg/mL.[33] According to biological evaluation of medical devices—Part 5: Tests for *in vitro* cytotoxicity (ISO 10993-5:2009), if cell viability of the material is less than 70%, then it has a cytotoxic potential. However, CPNPs and CIP-CPNP exhibit cell viability greater than 80% indicating that the as-synthesized samples are cytocompatible with primary cell polymorphonuclear.[27]

CONCLUSIONS

CPNPs in the phase of HAP could be successfully synthesized using the wet chemical precipitation method that was confirmed and FTIR. The size and morphology of the CPNPs were characterized by SEM analysis. The distorted spherical shape and average size of 28.02 ± 3.2 nm were confirmed through the SEM analysis. It is observed that 1:4 and 1:2 WR of CIP:CPNPs showed higher antibacterial activity against MDR bacteria, as compared to a 1:1 WR, indicating that the CIP:CPNPs' antibacterial activity increases with the decrement in CPNPs size and CIP concentration. Since the MTT assay of the bare CPNPs and CPNPs, in combination with CIP, recorded cell viability more than 80% for polymorphonuclear cells, CPNPs possess good bioactivity and acceptable toxicity that will make them a potential target for further medicinal and therapeutic application.

REFERENCES

1. Kalarikkal N, Augustine R, Oluwafemi OS, Joshy KS, Thomas S. Nanomedicine and Tissue Engineering: State of the Art and Recent Trends. CRC Press; 2016.
2. Theuretzbacher U. Antibiotic innovation for future public health needs. Clin Microbiol Infect. 2017;23(10):713–7.
3. Lopez-Carrizales M, Velasco K, Castillo C, Flores A, Magaña M, Martinez-Castanon G, et al. In Vitro Synergism of Silver Nanoparticles with Antibiotics as an Alternative Treatment in Multiresistant Uropathogens. Antibiotics. 2018;7(2):50.
4. Shaikh S, Nazam N, Rizvi SMD, Ahmad K, Baig MH, Lee EJ, et al. Mechanistic insights into the antimicrobial actions of metallic nanoparticles and their implications for multidrug resistance. Int J Mol Sci. 2019;20(10):2468.
5. Din FU, Aman W, Ullah I, Qureshi OS, Mustapha O, Shafique S, et al. Effective use of nanocarriers as drug delivery systems for the treatment of selected tumors. Int J Nanomedicine. 2017;12:7291–309.
6. Pokale P, Shende S, Gade A, Rai M. Biofabrication of calcium phosphate nanoparticles using the plant Mimusops elengi. Environ Chem Lett. 2014;12(3):393–299.
7. Epple M, Ganesan K, Heumann R, Klesing J, Kovtun A, Neumann S, et al. Application of calcium phosphate nanoparticles in biomedicine. J Mater Chem. 2010;20(1):18–23.
8. Utneja S, Talwar S, Nawal RR, Sapra S, Mittal M, Rajain A, et al. Evaluation of remineralization potential and mechanical properties of pit and fissure sealants fortified with nano-hydroxyapatite and nano-amorphous calcium phosphate fillers: An in vitro study. J Conserv Dent JCD. 2018;21(6):681.
9. Khan SA, Khan SB, Khan LU, Farooq A. Fourier Transform Infrared Spectroscopy : Fundamentals and Application in Functional Groups and Nanomaterials Characterization Fourier Transform Infrared Spectroscopy : Fundamentals and Application in Functional Groups and Nanomaterials Characterization. 2019;(February).
10. Heera P, Shanmugam S. Nanoparticle characterization and application: an overview. Int J Curr Microbiol App Sci. 2015;4(8):379–386.
11. Mndal S, Dey A, Pal U. Low temperature wet-chemical synthesis of spherical hydroxyapatite nanoparticles and their in situ cytotoxicity study. Adv Nano Res. 2016;4(4):295–307.
12. KHOSRAVI DK, Mozafari MR, Rashidi L, Mohammadi M. Calcium based non-viral gene delivery: an overview of methodology and applications. 2010;
13. Al-ubaidi GT. Nanomaterial in diagnosis and enhancement of cell mediated immune response to tuberculosis : In-vitro study. 2018;
14. Chandrasekar A, Sagadevan S, Dakshnamoorthy A. Synthesis and characterization of nano-hydroxyapatite (n-HAP) using the wet chemical technique. Int J Phys Sci. 2013;8(32):1639-1645.
15. Nithya R, Sundaram NM. Biodegradation and cytotoxicity of ciprof loxacin-loaded hydroxyapatite-polycaprolactone nanocomposite film for sustainable bone implants. Int J Nanomedicine. 2015;10(Suppl 1):119.
16. Kumar GS, Rajendran S, Karthi S, Govindan R, Girija EK, Karunakaran G, et al. Green synthesis and antibacterial activity of hydroxyapatite nanorods for orthopedic applications. MRS Commun. 2017;7(2):183–188.
17. Kojima S, Nagata F, Kugimiya S, Kato K. Synthesis of peptide-containing calcium phosphate nanoparticles exhibiting highly selective adsorption of various proteins. Appl Surf Sci. 2018;458:438–445.
18. Paz A, Guadarrama D, López M, E González J, Brizuela N, Aragón J. A comparative study of hydroxyapatite nanoparticles synthesized by different routes. Quim Nova. 2012;35(9):1724-1727.
19. Gayathri B, Muthukumarasamy N, Velauthapillai D, Santhosh SB. Magnesium incorporated hydroxyapatite nanoparticles: preparation, characterization, antibacterial and larvicidal activity. Arab J Chem. 2018;11(5):645–654.
20. Sahoo S, Chakraborti CK, Mishra SC, Nanda UN, Naik S. FTIR and XRD investigations of some fluoroquinolones. 2011.
21. Khurana C, Vala AK, Andhariya N, Pandey OP, Chudasama B. Influence of antibiotic adsorption on biocidal activities of silver nanoparticles. IET nanobiotechnology. 2016;10(2):69–74.
22. Kumar NA, Kumar S. Hydroxyapatite–ciprofloxacin minipellets for bone-implant delivery: preparation, characterization, in-vitro drug adsorption and dissolution studies. Int J Drug Deliv Res. 2009;1(1):47–59.

23. Kaur A, Kumar R. Enhanced bactericidal efficacy of polymer stabilized silver nanoparticles in conjugation with different classes of antibiotics. RSC Adv. 2019;9(2):1095–1105.
24. Maleki Dizaj S, Lotfipour F, Barzegar-Jalali M, Zarrintan M-H, Adibkia K. Ciprofloxacin HCl-loaded calcium carbonate nanoparticles: preparation, solid state characterization, and evaluation of antimicrobial effect against Staphylococcus aureus. Artif cells, nanomedicine, Biotechnol. 2017;45(3):535-543.
25. Jacoby GA. Mechanisms of resistance to quinolones. Clin Infect Dis. 2005;41(Supplement_2):S120–S126.
26. Ciocilteu M-V, Mocanu AG, Mocanu A, Ducu C, Nicolaescu OE, Manda VC, et al. Hydroxyapatite-ciprofloxacin delivery system: Synthesis, characterisation and antibacterial activity. Acta Pharm. 2018;68(2):129–144.
27. Kumar GS, Govindan R, Girija EK. In situ synthesis, characterization and in vitro studies of ciprofloxacin loaded hydroxyapatite nanoparticles for the treatment of osteomyelitis. J Mater Chem B. 2014;2(31):5052–5060.
28. Al-Bazaz FA-R, Radhi NJMH, Hubeatir KA. Sensitivity of Streptococcus Mutans to Selected Nanoparticles: In Vitro Study. J Baghdad Coll Dent. 2018;325(5817):1–7.
29. Wilson WW, Wade MM, Holman SC, Champlin FR. Status of methods for assessing bacterial cell surface charge properties based on zeta potential measurements. J Microbiol Methods. 2001;43(3):153–64.
30. Pan X, Chen S, Li D, Rao W, Zheng Y, Yang Z, et al. The synergistic antibacterial mechanism of gentamicin-loaded CaCO3 nanoparticles. Front Chem. 2018;5:130.
31. Elyerdi SMM, Sarvi MN, O'Connor AJ. Synthesis of ultra small nanoparticles (< 50 nm) of mesoporous MCM-48 for bio-adsorption. J Porous Mater. 2019;26(3):839-846.
32. Zhang J, Wang C, Wang J, Qu Y, Liu G. In vivo drug release and antibacterial properties of vancomycin loaded hydroxyapatite/chitosan composite. Drug Deliv. 2012;19(5):264–269.